Measurement of the Branching Fraction, Polarization, and CP Asymmetry for $B^0 \to \rho^+\rho^-$ Decays, and Determination of the Cabibbo-Kobayashi-Maskawa Phase ϕ_2

A. Somov,[4] A. J. Schwartz,[4] K. Abe,[7] K. Abe,[42] I. Adachi,[7] H. Aihara,[44] D. Anipko,[1] K. Arinstein,[1] Y. Asano,[48] V. Aulchenko,[1] T. Aushev,[12] T. Aziz,[40] S. Bahinipati,[4] A. M. Bakich,[39] V. Balagura,[12] A. Bay,[17] I. Bedny,[1] K. Belous,[11] U. Bitenc,[13] I. Bizjak,[13] S. Blyth,[23] A. Bondar,[1] A. Bozek,[26] M. Bračko,[7,19,13] J. Brodzicka,[26] T. E. Browder,[6] M.-C. Chang,[43] P. Chang,[25] Y. Chao,[25] A. Chen,[23] W. T. Chen,[23] B. G. Cheon,[3] R. Chistov,[12] S.-K. Choi,[5] Y. Choi,[38] Y. K. Choi,[38] A. Chuvikov,[33] S. Cole,[39] J. Dalseno,[20] M. Dash,[49] J. Dragic,[7] A. Drutskoy,[4] S. Eidelman,[1] D. Epifanov,[1] N. Gabyshev,[1] A. Garmash,[33] T. Gershon,[7] A. Go,[23] G. Gokhroo,[40] B. Golob,[18,13] K. Hara,[7] T. Hara,[30] N. C. Hastings,[44] K. Hayasaka,[21] H. Hayashii,[22] M. Hazumi,[7] Y. Hoshi,[42] S. Hou,[23] W.-S. Hou,[25] Y. B. Hsiung,[25] T. Iijima,[21] K. Ikado,[21] K. Inami,[21] A. Ishikawa,[7] H. Ishino,[45] R. Itoh,[7] M. Iwasaki,[44] Y. Iwasaki,[7] J. H. Kang,[50] P. Kapusta,[26] N. Katayama,[7] H. Kawai,[2] T. Kawasaki,[27] H. Kichimi,[7] H. J. Kim,[16] S. K. Kim,[37] S. M. Kim,[38] K. Kinoshita,[4] S. Korpar,[19,13] P. Križan,[18,13] P. Krokovny,[1] C. C. Kuo,[23] A. Kusaka,[44] A. Kuzmin,[1] Y.-J. Kwon,[50] G. Leder,[10] T. Lesiak,[26] J. Li,[36] A. Limosani,[7] S.-W. Lin,[25] J. MacNaughton,[10] F. Mandl,[10] D. Marlow,[33] T. Matsumoto,[46] W. Mitaroff,[10] K. Miyabayashi,[22] H. Miyake,[30] H. Miyata,[27] Y. Miyazaki,[21] R. Mizuk,[12] D. Mohapatra,[49] Y. Nagasaka,[8] M. Nakao,[7] Z. Natkaniec,[26] S. Nishida,[7] O. Nitoh,[47] S. Noguchi,[22] S. Ogawa,[41] T. Ohshima,[21] T. Okabe,[21] S. Okuno,[14] S. L. Olsen,[6] W. Ostrowicz,[26] H. Ozaki,[7] H. Palka,[26] C. W. Park,[38] H. Park,[16] R. Pestotnik,[13] L. E. Piilonen,[49] A. Poluektov,[1] Y. Sakai,[7] T. R. Sarangi,[7] N. Sato,[21] T. Schietinger,[17] O. Schneider,[17] C. Schwanda,[10] R. Seidl,[34] K. Senyo,[21] M. E. Sevior,[20] M. Shapkin,[11] H. Shibuya,[41] B. Shwartz,[1] V. Sidorov,[1] A. Sokolov,[11] N. Soni,[31] S. Stanič,[28] M. Starič,[13] T. Sumiyoshi,[46] S. Suzuki,[35] O. Tajima,[7] F. Takasaki,[7] K. Tamai,[7] N. Tamura,[27] M. Tanaka,[7] G. N. Taylor,[20] Y. Teramoto,[29] X. C. Tian,[32] K. Trabelsi,[6] T. Tsuboyama,[7] T. Tsukamoto,[7] S. Uehara,[7] T. Uglov,[12] K. Ueno,[25] Y. Unno,[7] S. Uno,[7] P. Urquijo,[20] Y. Ushiroda,[7] Y. Usov,[1] G. Varner,[6] S. Villa,[17] C. H. Wang,[24] M.-Z. Wang,[25] Y. Watanabe,[45] E. Won,[15] Q. L. Xie,[9] B. D. Yabsley,[39] A. Yamaguchi,[43] M. Yamauchi,[7] J. Ying,[32] L. M. Zhang,[36] Z. P. Zhang,[36] and V. Zhilich[1]

(Belle Collaboration)

[1]*Budker Institute of Nuclear Physics, Novosibirsk*
[2]*Chiba University, Chiba*
[3]*Chonnam National University, Kwangju*
[4]*University of Cincinnati, Cincinnati, Ohio 45221*
[5]*Gyeongsang National University, Chinju*
[6]*University of Hawaii, Honolulu, Hawaii 96822*
[7]*High Energy Accelerator Research Organization (KEK), Tsukuba*
[8]*Hiroshima Institute of Technology, Hiroshima*
[9]*Institute of High Energy Physics, Chinese Academy of Sciences, Beijing*
[10]*Institute of High Energy Physics, Vienna*
[11]*Institute of High Energy Physics, Protvino*
[12]*Institute for Theoretical and Experimental Physics, Moscow*
[13]*J. Stefan Institute, Ljubljana*
[14]*Kanagawa University, Yokohama*
[15]*Korea University, Seoul*
[16]*Kyungpook National University, Taegu*
[17]*Swiss Federal Institute of Technology of Lausanne, EPFL, Lausanne*
[18]*University of Ljubljana, Ljubljana*
[19]*University of Maribor, Maribor*
[20]*University of Melbourne, Victoria*
[21]*Nagoya University, Nagoya*
[22]*Nara Women's University, Nara*
[23]*National Central University, Chung-li*
[24]*National United University, Miao Li*
[25]*Department of Physics, National Taiwan University, Taipei*
[26]*H. Niewodniczanski Institute of Nuclear Physics, Krakow*
[27]*Niigata University, Niigata*
[28]*Nova Gorica Polytechnic, Nova Gorica*
[29]*Osaka City University, Osaka*

[30]Osaka University, Osaka
[31]Panjab University, Chandigarh
[32]Peking University, Beijing
[33]Princeton University, Princeton, New Jersey 08544
[34]RIKEN BNL Research Center, Upton, New York 11973
[35]Saga University, Saga
[36]University of Science and Technology of China, Hefei
[37]Seoul National University, Seoul
[38]Sungkyunkwan University, Suwon
[39]University of Sydney, Sydney, New South Wales
[40]Tata Institute of Fundamental Research, Bombay
[41]Toho University, Funabashi
[42]Tohoku Gakuin University, Tagajo
[43]Tohoku University, Sendai
[44]Department of Physics, University of Tokyo, Tokyo
[45]Tokyo Institute of Technology, Tokyo
[46]Tokyo Metropolitan University, Tokyo
[47]Tokyo University of Agriculture and Technology, Tokyo
[48]University of Tsukuba, Tsukuba
[49]Virginia Polytechnic Institute and State University, Blacksburg, Virginia 24061
[50]Yonsei University, Seoul

(Received 11 January 2006; published 2 May 2006)

We have measured the branching fraction $\mathcal{B}$, longitudinal polarization fraction f_L, and CP asymmetry coefficients $\mathcal{A}$ and $\mathcal{S}$ for $B^0 \to \rho^+\rho^-$ decays with the Belle detector at the KEKB e^+e^- collider using 253 fb^{-1} of data. We obtain $\mathcal{B} = [22.8 \pm 3.8(\text{stat})^{+2.3}_{-2.6}(\text{syst})] \times 10^{-6}$, $f_L = 0.941^{+0.034}_{-0.040}(\text{stat}) \pm 0.030(\text{syst})$, $\mathcal{A} = 0.00 \pm 0.30(\text{stat}) \pm 0.09(\text{syst})$, and $\mathcal{S} = 0.08 \pm 0.41(\text{stat}) \pm 0.09(\text{syst})$. These values are used to constrain the Cabibbo-Kobayashi-Maskawa phase ϕ_2; the solution consistent with the standard model is $\phi_2 = (88 \pm 17)^\circ$ or $59^\circ < \phi_2 < 115^\circ$ at 90% C.L.

DOI: 10.1103/PhysRevLett.96.171801 PACS numbers: 13.25.Hw, 11.30.Er, 12.15.Hh

One of the main goals of the e^+e^- "B factories" is to determine whether the Cabibbo-Kobayashi-Maskawa [1] mixing matrix with three quark generations is unitary; failure to satisfy this criterion would indicate new physics. Unitarity imposes six independent constraints upon the matrix elements, one of which is $V^*_{ub}V_{ud} + V^*_{cb}V_{cd} + V^*_{tb}V_{td} = 0$. Plotting this relationship in the complex plane yields a triangle, and unitarity is tested by measuring the internal angles (denoted ϕ_1, ϕ_2, ϕ_3) to check whether they sum to 180°. The angle ϕ_2 is the phase difference between $V^*_{tb}V_{td}$ and $-V^*_{ub}V_{ud}$ and is measured via $b \to u$ decays such as $B^0 \to \pi^+\pi^-$, $\rho^\pm\pi^\mp$, and $\rho^+\rho^-$ [2]. Of these, $B^0 \to \rho^+\rho^-$ gives the most precise value as the contribution from a possible loop amplitude (with a different weak phase) is smallest. The size of the loop amplitude is constrained by the upper limit on $\mathcal{B}(B^0 \to \rho^0\rho^0)$ [3].

One determines ϕ_2 by measuring the Δt distributions of $B^0\bar{B}^0$ events, where Δt is the difference between the decay time of the signal $B^0(\bar{B}^0)$ and that of the opposite-side $\bar{B}^0(B^0)$. For $B^0/\bar{B}^0 \to \rho^+\rho^-$ decays, these distributions have interference terms of opposite sign proportional to $e^{-|\Delta t|/\tau_{B^0}}[\mathcal{A}\cos(\Delta m \Delta t) + \mathcal{S}\sin(\Delta m \Delta t)]$, where Δm is the $B^0 - \bar{B}^0$ mass difference and $\mathcal{A}$, $\mathcal{S}$ are functions of ϕ_2. Here we present a measurement of the $B^0 \to \rho^+\rho^-$ branching fraction $\mathcal{B}$, longitudinal polarization fraction f_L, and coefficients $\mathcal{A}$ and $\mathcal{S}$, using 253 fb^{-1} of data recorded by the Belle experiment [4] at KEKB [5].

Candidate $B^0 \to \rho^+\rho^-$, $\rho^\pm \to \pi^\pm\pi^0$ decays are selected by requiring two oppositely charged tracks satisfying $p_T > 0.10$ GeV/c, $dr < 0.2$ cm, and $|dz| < 4.0$ cm, where p_T is the momentum transverse to the beam axis, and dr and dz are the radial and longitudinal distances, respectively, between the track and the beam crossing point. The tracks are fitted to a common vertex. We require that tracks be identified as pions based on information from a time-of-flight system, an aerogel Čerenkov counter system, and the central tracker [4]. The resulting identification efficiency is about 89%, and the kaon misidentification rate is about 10%. Tracks are rejected if they satisfy an electron identification criterion based on information from an electromagnetic calorimeter (ECL).

The $\pi^\pm$ candidates are combined with π^0 candidates reconstructed from γ pairs having $M_{\gamma\gamma}$ in the range 117.8–150.2 MeV/c^2 ($\pm 3\sigma$ in m_{π^0} resolution). We require $E_\gamma > 50(90)$ MeV in the ECL barrel (end cap), which subtends 32°–129° (17°–32° and 129°–150°) with respect to the beam axis. To identify $\rho^\pm \to \pi^\pm\pi^0$ decays, we require that $M_{\pi^\pm\pi^0}$ be in the range 0.62–0.92 GeV/c^2 ($\pm 2\Gamma$ in the $M_{\pi^\pm\pi^0}$ distribution). To reduce combinatorial background, the π^0's must have $p > 0.35$ GeV/c in the e^+e^- center-of-mass (c.m.) frame, and $\rho^\pm$ candidates must satisfy $-0.80 < \cos\theta_\pm < 0.98$, where $\theta_\pm$ is the angle between the direction of the π^0 from the $\rho^\pm$ and the negative of the B^0 momentum in the $\rho^\pm$ rest frame.

To identify $B^0 \to \rho^+\rho^-$ decays, we calculate variables $M_{\rm bc} \equiv \sqrt{E^2_{\rm beam} - p^2_B}$ and $\Delta E \equiv E_B - E_{\rm beam}$, where E_B and p_B are the reconstructed energy and momentum of the B candidate, and $E_{\rm beam}$ is the beam energy, all evaluated in the c.m. frame. The ΔE distribution has a tail on the lower side due to incomplete containment of the electromagnetic shower in the ECL. We define a signal region $M_{\rm bc} \in (5.27, 5.29)$ GeV/c^2 and $\Delta E \in (-0.12, 0.08)$ GeV.

We determine whether a B^0 or $\bar{B}^0$ evolved and decayed to $\rho^+\rho^-$ by tagging the b flavor of the nonsignal (opposite-side) B decay in the event. This is done using a tagging algorithm [6] that categorizes charged leptons, kaons, and Λ's found in the event. The algorithm returns two parameters: q, which equals $+1(-1)$ when the opposite-side B is most likely a $B^0(\bar{B}^0)$, and r, which indicates the tag quality as determined from Monte Carlo (MC) simulation and varies from $r = 0$ for no flavor discrimination to $r = 1$ for unambiguous flavor assignment.

The dominant background is $e^+e^- \to q\bar{q}(q = u, d, s, c)$ production. We discriminate against this using event topology: $e^+e^- \to q\bar{q}$ events tend to be jetlike in the c.m. frame, while $e^+e^- \to B\bar{B}$ tends to be spherical. To quantify sphericity, we calculate 16 modified Fox-Wolfram moments and combine them into a Fisher discriminant [7]. We calculate a probability density function (PDF) for this discriminant and multiply it by a PDF for $\cos\theta_B$, where θ_B is the polar angle in the c.m. frame between the B direction and the beam axis. $B\bar{B}$ events have a $1 - \cos^2\theta_B$ distribution, while $q\bar{q}$ events tend to be uniform in $\cos\theta_B$. The PDFs for signal and $q\bar{q}$ are obtained from MC simulation and a sideband [$M_{\rm bc} \in (5.21, 5.26)$ GeV/c^2], respectively. These PDFs are used to calculate a signal likelihood $\mathcal{L}_s$ and $q\bar{q}$ likelihood $\mathcal{L}_{q\bar{q}}$, and we require that $\mathcal{R} = \mathcal{L}_s/(\mathcal{L}_s + \mathcal{L}_{q\bar{q}})$ be above a threshold. As the tagging parameter r also discriminates against $q\bar{q}$ events, we divide the data into six r intervals (denoted $\ell = 1$–6) and determine the $\mathcal{R}$ threshold separately for each.

The overall efficiency (from MC simulation) is $(3.19 \pm 0.02)\%$. This value corresponds to $f_L = 1$; the change in efficiency $(+5.0\%)$ for f_L equal to its central value measured below is taken as a systematic error. The fraction of events having multiple candidates is 9.5%; most of these arise from fake π^0's combining with good tracks, and thus we choose the best candidate based on $|M_{\gamma\gamma} - m_{\pi^0}|$. In MC simulation this correctly identifies the $B^0 \to \rho^+\rho^-$ decay about 90% of the time. A small fraction of signal decays (5.7% for longitudinal polarization) have $\geq 1\pi^\pm$ daughters incorrectly identified but pass all selection criteria; these are referred to as "self-cross-feed" (SCF) events. Their vertex positions (and hence Δt values) are smeared.

We determine the signal yield using two unbinned maximum likelihood (ML) fits. We first fit the $M_{\rm bc} - \Delta E$ distribution in the wide range $M_{\rm bc} \in (5.21, 5.29)$ GeV/c^2 and $\Delta E \in (-0.20, 0.30)$ GeV to obtain the $B^0 \to (\rho^+\rho^- +$ nonresonant) yield $N_{(\rho\rho+{\rm nr})}$; we then fit the $M_{\pi^\pm\pi^0}$ distribution of events in the $M_{\rm bc} - \Delta E$ signal region to obtain the nonresonant $\rho^\pm\pi^\mp\pi^0 + \pi^\pm\pi^\mp\pi^0\pi^0$ fraction.

For the first fit we include PDFs for signal $\rho^+\rho^-$ and $b \to c$, $b \to u$, and $q\bar{q}$ backgrounds. The PDFs for signal and $b \to u$ are two-dimensional distributions obtained from MC simulation; the PDF for $b \to c$ is the product of a threshold ("ARGUS" [8]) function for $M_{\rm bc}$ and a quadratic polynomial for ΔE, also obtained from MC simulation. The PDF for $q\bar{q}$ is an ARGUS function for $M_{\rm bc}$ and a linear function for ΔE; the latter's slope depends on the tag quality bin ℓ. All $q\bar{q}$ shape parameters are floated in the fit. The $b \to u$ background is dominated by $B \to (\rho\pi, a_1\pi, a_1\rho)$ decays; as their contributions are small, their normalization is fixed to that from MC simulation. For $B^+ \to a_1^+\pi^0$ and $B \to a_1\rho$ modes, the branching fractions (unmeasured) used in the simulations are 3×10^{-5} and 2×10^{-5}, respectively; we vary these by $\pm 50\%$ and $\pm 100\%$, respectively, to obtain the systematic error due to these estimates. The result of the fit is $N_{(\rho\rho+{\rm nr})} = 207^{+28}_{-29}$ events. Figure 1 shows the final event sample and projections of the fit.

For the subsequent fit, we require that events be in the $M_{\rm bc} - \Delta E$ signal region and fit $M_{\pi^\pm\pi^0}$ in the wide range 0.30–1.80 GeV/c^2. One ρ candidate is required to satisfy $M_{\pi\pi^0} \in (0.62, 0.92)$ GeV/c^2; the mass of the other ρ candidate is then fit. We include additional PDFs for nonresonant $B \to \rho\pi\pi$ and $B \to \pi\pi\pi\pi$ decays; these are taken from MC simulation assuming three- and four-body phase space distributions. However, the fit result for $\pi\pi\pi\pi$ is $\ll 1\%$ and thus we set this fraction to zero. The PDFs for $\rho^+\rho^-$ and $b \to u$ are also taken from MC simulation. The PDFs for $b \to c$ and $q\bar{q}$ are combined and taken from the sideband $M_{\rm bc} \in (5.22, 5.26)$ GeV/c^2; we check with MC simulation that the shapes of these backgrounds and their ratio in the sideband region are close to those in the signal region. We impose the constraint that the fraction of $(\rho^+\rho^- + \rho\pi\pi)$ events in the $M_{\pi^\pm\pi^0}$ range 0.62–0.92 GeV/c^2 equals that obtained from the

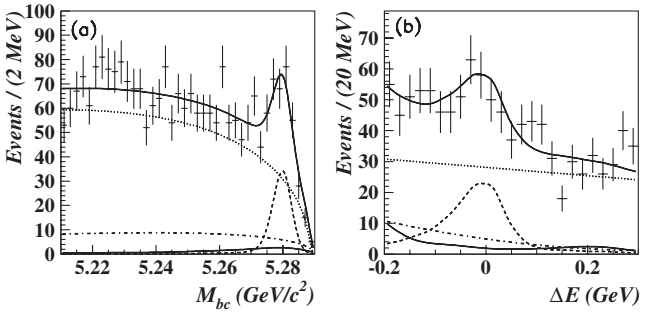

FIG. 1. (a) $M_{\rm bc}$ for events with $\Delta E \in (-0.10, 0.06)$ GeV. (b) ΔE for $M_{\rm bc} \in (5.27, 5.29)$ GeV/c^2. The curves show fit projections: the dashed curve is $\rho^+\rho^- + \rho\pi\pi$, the dotted curve is $q\bar{q}$, the dot-dashed curve is $b \to c$, the small solid curve is $b \to u$, and the large solid curve is the total.

$M_{\rm bc} - \Delta E$ fit; there is then only one free parameter. The fit obtains $\tilde{f}_{\rho\pi\pi} \equiv f_{\rho\pi\pi}/(f_{\rho\rho} + f_{\rho\pi\pi}) = (6.3 \pm 6.7)\%$, and thus $N_{\rho\rho} = (1 - \tilde{f}_{\rho\pi\pi})N_{(\rho\rho+{\rm nr})} = 194 \pm 32$, where the error is statistical and obtained from a "toy" MC study (since the errors on $\tilde{f}_{\rho\pi\pi}$ and $N_{(\rho\rho+{\rm nr})}$ are correlated). This value agrees well with the $\rho^+\rho^-$ yield obtained from the $M_{\pi\pi^0}$ fit (141 events) multiplied by the ratio of acceptances (1.33). Figure 2(a) shows the data and projections of the fit.

The branching fraction is $N_{\rho\rho}/(\varepsilon\varepsilon_\pi N_{B\bar{B}})$, where $N_{\rho\rho}$ is the number of $B^0 \to \rho^+\rho^-$ candidates, $N_{B\bar{B}}$ is the number of $B\bar{B}$ pairs produced [$(274.8 \pm 3.1) \times 10^6$], ε is the acceptance and event selection efficiency obtained from MC simulation, and ε_π is a correction factor for the $\pi^\pm$ identification requirement to account for small differences between data and the simulation (0.969 ± 0.012). The result is $\mathcal{B} = (22.8 \pm 3.8) \times 10^{-6}$, where the error is statistical.

There are 11 main sources of systematic error. These are typically evaluated by varying the relevant parameter(s) by 1σ and noting the change in $\mathcal{B}$. The sources are as follows: track reconstruction efficiency (1.2% per track); π^0 efficiency (4% per π^0); calibration factors (obtained from a large $B^+ \to \bar{D}^0\rho^+ \to K^+\pi^-\pi^0\rho^+$ sample) used to correct the signal $M_{\rm bc} - \Delta E$ PDF to better match the data; the $M_{\rm bc} - \Delta E$ shapes for $b \to c$; the fraction and $M_{\rm bc} - \Delta E$ shapes for $b \to u$; the ΔE range fit; statistics of the MC simulation used to calculate ε; the dependence of ε upon the polarization; uncertainties in ε_π and $N_{B\bar{B}}$; and the $q\bar{q}$ suppression requirement. Combining these in quadrature gives a total systematic error of $+10.1\%$ and -11.6%. Thus,

$$\mathcal{B}_{B\to\rho^+\rho^-} = [22.8 \pm 3.8({\rm stat})^{+2.3}_{-2.6}({\rm syst})] \times 10^{-6}. \quad (1)$$

To determine the longitudinal polarization fraction f_L, we perform an unbinned ML fit to the θ_+, θ_- helicity angle distribution. This distribution is proportional to $[4f_L\cos^2\theta_+\cos^2\theta_- + (1 - f_L)\sin^2\theta_+\sin^2\theta_-]$. In the fit, this PDF is multiplied by an acceptance function determined from MC simulation. The acceptance is modeled as the product $A(\cos\theta_+) \cdot A(\cos\theta_-)$, where A is a polynomial.

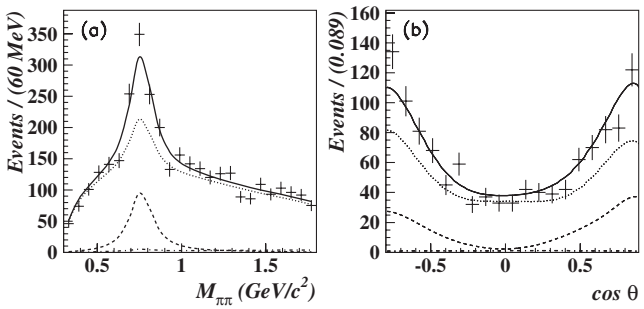

FIG. 2. (a) $M_{\pi^\pm\pi^0}$ for events in the $M_{\rm bc} - \Delta E$ signal region that satisfy $M_{\pi\pi^0}$(not fit) $\in (0.62, 0.92)$ GeV/c^2. (b) Sum of $\cos\theta_\pm$ distributions for events in the signal region that satisfy $M_{\pi^\pm\pi^0}$(both) $\in (0.62, 0.92)$ GeV/c^2. The curves show fit projections: the dashed curve is $\rho^+\rho^-$, the dot-dashed curve is $\rho\pi\pi$, the dotted curve is $q\bar{q} + (b \to c) + (b \to u)$, and the solid curve is the total.

We fit events in the $M_{\rm bc} - \Delta E$ signal region that satisfy $M_{\pi^\pm\pi^0} \in (0.62, 0.92)$ GeV/c^2. We include PDFs for signal, $\rho\pi\pi$, and $b \to c$, $b \to u$, and $q\bar{q}$ backgrounds. The PDFs for $b \to c$ and $q\bar{q}$ are combined and determined from the sideband $M_{\rm bc} \in (5.21, 5.26)$ GeV/c^2, $\Delta E \in (-0.12, 0.12)$ GeV; we check with MC simulation that the shapes of these backgrounds and their ratio in the sideband region are close to those in the signal region. The PDF for $b \to u$ is taken from MC simulation. The fraction of $\rho^+\rho^- + \rho\pi\pi$ is taken from the $M_{\rm bc} - \Delta E$ fit; the component $f_{\rho\pi\pi}$ alone is taken from the $M_{\pi^\pm\pi^0}$ fit. The fraction of $b \to u$ background is small and taken from MC simulation. Since $f_{(q\bar{q}+b\to c)} = 1 - f_{\rho\rho} - f_{\rho\pi\pi} - f_{b\to u}$, there is only one free parameter in the fit. The result is $f_L = 0.941^{+0.034}_{-0.040}$, where the error is statistical. Figure 2(b) shows the data and projections of the fit.

There are eight main sources of systematic error in f_L: the $\rho^+\rho^- + \rho\pi\pi$ fraction $(+0.013, -0.012)$; the $\rho\pi\pi$ component alone $(+0.021, -0.020)$; the pion identification efficiency, which affects the acceptance $(+0.000, -0.004)$; misreconstructed $B^0 \to \rho^+\rho^-$ decays $(+0.005, -0.000)$; the $q\bar{q}$ suppression requirement (± 0.013); interference of longitudinally polarized ρ's with an S-wave $\pi^\pm\pi^0$ system in $B^0 \to \rho\pi\pi$ $(+0.003, -0.005)$; a very small bias in the fitting procedure measured from a large toy MC sample $(+0.000, -0.005)$; and uncertainty in the $q\bar{q} + (b \to c)$ background shape $(+0.004, -0.014)$. This last uncertainty is evaluated by taking the background shape from alternative $M_{\rm bc}$, ΔE sidebands. Combining all errors in quadrature gives a total systematic error of ± 0.030. Thus,

$$f_L = 0.941^{+0.034}_{-0.040}({\rm stat}) \pm 0.030({\rm syst}). \quad (2)$$

To determine CP coefficients $\mathcal{A}$ and $\mathcal{S}$, we divide the data into $q = \pm 1$ tagged subsamples and do an unbinned ML fit to their Δt distributions. Since B^0's and $\bar{B}^0$'s are approximately at rest in the $\Upsilon(4S)$ frame, and the $\Upsilon(4S)$ travels with $\beta\gamma = 0.425$ nearly along the beam axis (z), Δt is determined from the z displacement between the $\rho^+\rho^-$ and tag-side decay vertices: $\Delta t \approx (z_{CP} - z_{\rm tag})/\beta\gamma c$.

The likelihood function for event i is a sum of terms:

$$\mathcal{L}_i = f^{(i)}_{\rho\rho}\mathcal{P}(\Delta t)_{\rho\rho} + f^{(i)}_{\rm SCF}\mathcal{P}(\Delta t)_{\rm SCF} + f^{(i)}_{\rho\pi\pi}\mathcal{P}(\Delta t)_{\rho\pi\pi} + f^{(i)}_{b\to c}\mathcal{P}(\Delta t)_{b\to c} + f^{(i)}_{b\to u}\mathcal{P}(\Delta t)_{b\to u} + f^{(i)}_{q\bar{q}}\mathcal{P}(\Delta t)_{q\bar{q}},$$

where the weights $f^{(i)}$ are functions of $M_{\rm bc}$ and ΔE and are normalized to the event fractions obtained from the $M_{\rm bc} - \Delta E$ and $M_{\pi^\pm\pi^0}$ fits. The PDFs $\mathcal{P}(\Delta t)$ are obtained from MC simulation for $b \to c$ and $b \to u$ and from an $M_{\rm bc}$ sideband for $q\bar{q}$. We include a term for SCF events in

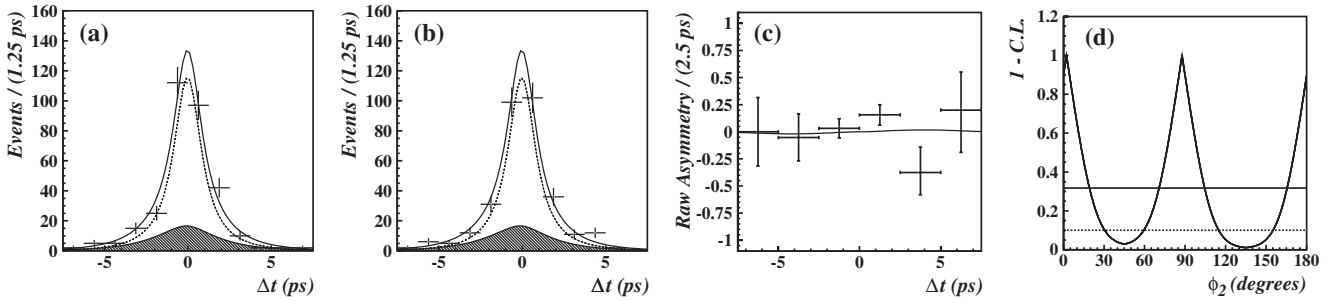

FIG. 3. The Δt distribution of events in the $M_{\rm bc} - \Delta E$ signal region that satisfy $M_{\pi^\pm\pi^0} \in (-0.62, 0.92)$ GeV/c^2, and projections of the fit. (a) $q = +1$ tags; (b) $q = -1$ tags; (c) raw CP asymmetry for good tags ($0.5 < r < 1.0$); (d) $1 -$ C.L. vs ϕ_2. In (a), the hatched region (dashed line) shows signal (background) events. In (d), the solid (dashed) horizontal line denotes C.L. = 68.3% (90%).

which a $\pi^\pm$ daughter is swapped with a tag-side track; the PDF and function $f_{\rm SCF}$ are also obtained from MC simulation.

The signal PDF is $e^{-|\Delta t|/\tau_{B^0}}/(4\tau_{B^0})\{1 \mp \Delta\omega_\ell \pm (1 - 2\omega_\ell)[\mathcal{A}\cos(\Delta m\Delta t) + \mathcal{S}\sin(\Delta m\Delta t)]\}$, where the upper (lower) sign corresponds to $B^0(\bar{B}^0)$ tags, ω_ℓ is the mistag fraction for the ℓth bin of tagging parameter r, and $\Delta\omega_\ell$ is a possible difference in ω_ℓ between B^0 and $\bar{B}^0$ tags. Values of ω_ℓ and $\Delta\omega_\ell$ are determined from a large $B^0 \to D^{*-}\ell^+\nu$ sample. Coefficients $\mathcal{A}$ and $\mathcal{S}$ receive contributions from longitudinally (L) and transversely (T) polarized amplitudes, e.g., $\mathcal{A} = f_L\mathcal{A}_L + (1 - f_L)\mathcal{A}_T$. The transversely polarized amplitude has a CP-odd component. For a negligible penguin contribution, $\mathcal{A}_T = \mathcal{A}_L$ but $\mathcal{S}_T = [(1 - f_L - 2f_{CP-\rm odd})/(1 - f_L)]\mathcal{S}_L$; since $f_{CP\text{-odd}} \leq f_T$ and f_T is small, we assume $\mathcal{A} = \mathcal{A}_L$, $\mathcal{S} = \mathcal{S}_L$, and take the possible difference as a systematic error.

The signal PDF is convolved with the same Δt resolution function as that used for Belle's $\sin 2\phi_1$ measurement [9]. The PDFs $\mathcal{P}_{\rho\pi\pi}$ and $\mathcal{P}_{\rm SCF}$ are exponential with $\tau = \tau_B$ and $\tau \approx 0.93$ ps (from MC simulation), respectively; these are smeared by a common resolution function. We determine $\mathcal{A}$ and $\mathcal{S}$ by maximizing $\sum_i \log\mathcal{L}_i$, where i runs over the 656 events in the $M_{\rm bc} - \Delta E$ signal region that satisfy $M_{\pi^\pm\pi^0} \in (0.62, 0.92)$ GeV/c^2. The results are $\mathcal{A} = 0.00 \pm 0.30$ and $\mathcal{S} = 0.08 \pm 0.41$, where the errors are statistical. The correlation coefficient is -0.057. These values are consistent with no CP violation ($\mathcal{A} = \mathcal{S} = 0$); the errors are consistent with expectations based on MC simulation. Figure 3 shows the data and projections of the fit.

The sources of systematic error are listed in Table I. The error due to wrong-tag fractions is evaluated by varying ω_ℓ and $\Delta\omega_\ell$ values. The effect of a possible asymmetry in $b \to c$ and $q\bar{q}$ is evaluated by adding such an asymmetry to the $b \to c$ and $q\bar{q}$ Δt distributions. The error due to transverse polarization is obtained by first setting f_L equal to its central value and varying $\mathcal{A}_T$, $\mathcal{S}_T$ from -1 to $+1$, then assuming $\mathcal{A}_T = \mathcal{A}_L$, $\mathcal{S}_T = -\mathcal{S}_L$ (f_T is CP odd), and varying f_L by its error. The sum in quadrature of all systematic errors is ± 0.09. Thus,

$$\mathcal{A}_L = 0.00 \pm 0.30(\text{stat}) \pm 0.09(\text{syst}), \quad (3)$$

$$\mathcal{S}_L = 0.08 \pm 0.41(\text{stat}) \pm 0.09(\text{syst}). \quad (4)$$

These values are similar to those obtained by *BABAR* [11].

We use these values and the branching fractions for $B^0 \to \rho^+\rho^-$ [12], $\rho^+\rho^0$ [13], and $\rho^0\rho^0$ [3] to constrain ϕ_2. We assume isospin symmetry [14] and follow Ref. [15], neglecting a possible $I = 1$ contribution to $B^0 \to \rho^+\rho^-$ [16]. We first fit the measured values to obtain a minimum χ^2 (denoted $\chi^2_{\rm min}$); we then scan ϕ_2 from 0° to 180°, calculating the difference $\Delta\chi^2 \equiv \chi^2(\phi_2) - \chi^2_{\rm min}$. We insert $\Delta\chi^2$ into the cumulative distribution function for the χ^2 distribution for 1 degree of freedom to obtain a confidence level (C.L.) for each ϕ_2 value. The resulting function $1 -$ C.L. [Fig. 3(d)] has more than one peak due to ambiguities that arise when solving for ϕ_2. However, only one solution is consistent with the standard model [13]: $(88 \pm 17)°$ or $59° < \phi_2 < 115°$ at 90% C.L.

In summary, using 253 fb^{-1} of data we have measured the branching fraction, polarization fraction, and CP coefficients $\mathcal{A}$ and $\mathcal{S}$ for $B^0 \to \rho^+\rho^-$ decays, and constrained the angle ϕ_2.

TABLE I. Systematic errors for CP coefficients $\mathcal{A}$ and $\mathcal{S}$.

Type	$\Delta\mathcal{A}(\times 10^{-2})$ $+\sigma$	$-\sigma$	$\Delta\mathcal{S}(\times 10^{-2})$ $+\sigma$	$-\sigma$
Wrong-tag fractions	0.5	0.6	0.8	0.8
Parameters Δm, τ_{B^0}	0.1	0.1	0.9	0.9
Resolution function	1.3	1.3	1.3	1.3
Background Δt distributions	1.6	1.5	2.3	2.5
Component fractions	2.1	2.6	5.1	4.5
Background asymmetry	0.0	2.0	0.0	4.3
Possible fitting bias	0.0	1.0	0.7	0.0
Vertexing	4.1	2.8	1.3	1.4
Tag-side interference [10]	3.7	3.7	0.1	0.1
Transverse polarization	6.3	6.3	7.1	5.8
Total	+8.9	−8.8	+9.3	−9.2

We thank the KEKB group for the excellent operation of the accelerator, the KEK cryogenics group for the efficient operation of the solenoid, and the KEK computer group and the NII for valuable computing and Super-SINET network support. We acknowledge support from MEXT and JSPS (Japan); ARC and DEST (Australia); NSFC (Contract No. 10175071, China); DST (India); the BK21 program of MOEHRD and the CHEP SRC program of KOSEF (Korea); KBN (Contract No. 2P03B 01324, Poland); MIST (Russia); MESS (Slovenia); NSC and MOE (Taiwan); and DOE (USA).

[1] M. Kobayashi and T. Maskawa, Prog. Theor. Phys. **49**, 652 (1973); N. Cabibbo, Phys. Rev. Lett. **10**, 531 (1963).
[2] Charge-conjugate modes are included throughout this Letter unless noted otherwise.
[3] B. Aubert *et al.* (*BABAR* Collaboration), Phys. Rev. Lett. **94**, 131801 (2005).
[4] A. Abashian *et al.*, Nucl. Instrum. Methods Phys. Res., Sect. A **479**, 117 (2002).
[5] S. Kurokawa and E. Kikutani, Nucl. Instrum. Methods Phys. Res., Sect. A **499**, 1 (2003), and other papers in this volume.
[6] H. Kakuno *et al.*, Nucl. Instrum. Methods Phys. Res., Sect. A **533**, 516 (2004).
[7] S. H. Lee *et al.* (Belle Collaboration), Phys. Rev. Lett. **91**, 261801 (2003).
[8] H. Albrecht *et al.* (ARGUS Collaboration), Phys. Lett. B **241**, 278 (1990).
[9] K.-F. Chen *et al.* (Belle Collaboration), Phys. Rev. D **72**, 012004 (2005).
[10] O. Long *et al.*, Phys. Rev. D **68**, 034010 (2003).
[11] B. Aubert *et al.* (*BABAR* Collaboration), Phys. Rev. Lett. **95**, 041805 (2005); **93**, 231801 (2004).
[12] We average our measurement with that of B. Aubert *et al.* (*BABAR* Collaboration), Phys. Rev. Lett. **93**, 231801 (2004).
[13] S. Eidelman *et al.* (Particle Data Group), Phys. Lett. B **592**, 1 (2004).
[14] M. Gronau and D. London, Phys. Rev. Lett. **65**, 3381 (1990).
[15] J. Charles *et al.* (CKMfitter Group), Eur. Phys. J. C **41**, 1 (2005).
[16] A. Falk *et al.*, Phys. Rev. D **69**, 011502(R) (2004).